

# Techno-Economic Optimization of Diffuser Configuration Effect on Centrifugal Compressor Performance

Waleed Al-Busaidi<sup>1,\*</sup>, Pericles Pilidis<sup>2</sup>

<sup>1</sup>Researcher in Cranfield University, Bedford, UK

<sup>2</sup>Head of Propulsion Engineering Centre, Cranfield University, Bedford, UK

\*Corresponding author: w.albusaidi@cranfield.ac.uk

**Abstract** Extensive research has been conducted on centrifugal compressors to investigate the influence of diffuser features on the stage performance. However, there are several geometrical parameters affecting the diffuser performance and the unsteady interaction with the rotating impeller which makes the appropriate selection of the optimum features more complex. Furthermore, the trade-off between the efficiency improvement and operating range extension necessitates the need for an optimization tool to decide the typical diffuser configuration. Hence, this paper aims to introduce a multi-decision optimization approach to define the overall diffuser characteristics based on the specified duty requirements. This approach uses the most recent developed models in this field to evaluate the impact of different diffuser types on the overall stage performance technically and economically. From the performance perspective, the influences of diffuser geometry have been utilized to study the impact on stage efficiency and stable flow range. Furthermore, this has been also discussed economically as a function of the diffuser losses cost in order to make the typical decision.

**Keywords:** centrifugal compressor, diffuser characteristics, optimization, multi-decision process

**Cite This Article:** Waleed Al-Busaidi, and Pericles Pilidis, "Techno-Economic Optimization of Diffuser Configuration Effect on Centrifugal Compressor Performance." *American Journal of Energy Research*, vol. 3, no. 2 (2015): 37-48. doi: 10.12691/ajer-3-2-4.

## 1. Introduction

An efficient diffusion system is a basic requirement to achieve a high performance of a centrifugal compressor stage over a wide flow range. However, there are several mechanical and aerodynamic limitation for the diffusion process in order to avoid the chance of the stall initiation. The conducted experimental and numerical studies revealed that the diffuser features have significant influence on the location of stability limit of the centrifugal compressor depending on the impeller design and its matching with the diffuser component. A higher overall efficiency can be accomplished by improving the pressure recovery of the diffuser.

Three basic types of diffuser have been developed to meet the required demand of more advanced machines with high operating efficiency and wide stable range which are: vaneless diffuser (VLD), conventional vaned diffuser (CVD) and low solidity vaned diffuser (LSVD). The vaneless diffuser is used frequently in process and turbocharger centrifugal compressors. It is less expensive than the rest of configurations and a reasonable static pressure coefficient can be achieved by the appropriate design diffuser. The performance of vaneless diffusers has been investigated theoretically and numerically by numerous researches including: Schumann [1], Yingkang

and Sjolander [2], Aungier[3], Tsujimoto et al. [4], Dou and Mizuki [5], Yu-Tai Lee et al. [6], Ljevar et al. [7], Gao et al. [8], Tamaki [9] and Kalinkevych et al. [10]. Moreover, several experimental studies have been carried out to demonstrate the impact of geometrical parameters on the stage performance such as: Abdelhamid [11], Kinoshita and Senoo [12] and Jaatinen-Varri et al. [13].

A higher operation efficiency of centrifugal compressor can be achieved by improving the pressure recovery of the diffusion system. It is generally found that a well-designed vaned diffuser has higher static pressure recovery coefficient ( $C_{pd}$ ) leading to a greater operating efficiency. However, the presence of vanes limits the available flow area and causes substantial changes in the steady flow field which in turn results in a shorter operating margin. The surge flow coefficient of conventional vaned diffusers (CVD) is highly affected by the initiated vane stall due to flow incidence. Aungier[14] concluded that the vaned diffuser stall in the centrifugal compressor stages with a pressure ratio above 1.7 is followed closely by stage surge.

Despite that it is often possible to design a conventional vaned diffuser (CVD) with a quite close choke limit to that of the impeller, this will be also in expenses of surge margin reduction and this limit is commonly controlled by the vaned diffuser features. There are extensive number of studies has been performed on the influences of vaned diffusers characteristics on stage performance such as: Yoshinaga et al. [15], Rodgers [16], Haupt et al. [17], Kim

and Engeda [18], Justen et al. [19], He and Tourlidakis [20], Kim et al. [21], Engeda [22], Turunen-Saaresti [23], Issac et al. [24], Kalinkevych et al. [25,26] and Reddy et al. [27].

The increase in the utilization of centrifugal compressors for various purposes necessitates the need for wider flow range and high stage efficiency. This in turn led to introduce the concept of low solidity vane diffuser (LSVD) by eliminating geometric throat. An improvement in the stage efficiency of the low solidity vane diffuser (LSVD) was achieved over vaneless diffusers (VLD) with lower reduction in the flow range comparing with conventional vane diffusers (CVD). The absence of a vane geometric throat in low solidity vane diffuser (LSVD) allows the stage to operate out to its impeller choke flow limit. However, this difference in the operating range may be small if impeller inducer is controlling the surge flow. Therefore, it is always a necessary to evaluate the relative merits of both the LSVD and the CVD in order to achieve the optimum performance based on the desired design requirements. Osborne and Sorokes [28] demonstrated experimentally a significant improvement in the performance of LSVD above a vaneless diffuser for designs covering a wider range of specific speed. Sorokes and Welch [29] studied the effects of setting angles on both diffuser and overall stage performance. Further investigation was conducted on rotatable LSVD by Sorokes and Welch [30].

However, this no existing approach in the literature to optimize the diffuser characteristics based on technical and economic perspective. Hence, this paper aims to introduce an approach to evaluate the diffuser geometrical features in order to select the optimum characteristics for the required process. In order to achieve that, three basic parameters have been analysed which are: stage efficiency, operating range and power loss cost.

## 2. Background to Developed Approach

The open literature revealed five main design parameters which have significant impact on the overall performance of the diffuser which are: diffuser width, radius ratio, chord length, vanes number and inlet vane angle. Kalinkevych et al. [25] proposed a method to calculate the flow parameters and energy characteristics of vaneless diffuser based on the boundary-layer theory. The flow was assumed to be steady state and circumferentially uniform and inlet velocities were assumed to be invariable by the width of the diffuser. Galerkin et al. [31] derived a new model to account the loss coefficient of vaneless diffuser. The basic principle of this model is based on the fact that the loss coefficient ( $\xi$ ) is a function of friction coefficient ( $\lambda_{fr}$ ), diameter ratio ( $D_4/D_3$ ), flow angle ( $\alpha_3$ ) and inlet diffuser width ( $b_3$ ).

$$\xi = \lambda_{fr} \left[ \frac{\left(1 - \frac{1}{D_4/D_3}\right)}{4 \frac{b_3}{D_3} \sin \alpha_3} \right] \quad (1)$$

$$\lambda_{fr} = \frac{0.316 X_2}{Re_3^{0.25}} + \left( \frac{45^\circ - \alpha_3}{35^\circ} \right)^{X_1} \times \left[ 0.012 + 0.314 \left( \frac{b_3}{D_3} - 0.014 \right) - \frac{0.316 X_2}{Re_3^{0.25}} \right] \quad (2)$$

Where:

$X_1, X_2$ : Empirical coefficients.

The diffuser width is defined based on the exit impeller geometry and the type of the diffuser inlet configuration (pinched, un-pinched). The estimation of the impeller exit width ( $b_2$ ) is critical for performance estimation and basic dimension setup due to its significant impact on flow coefficient and stage pressure ratio. Xu and Ryoichi [32] derived a simple correlation for this purpose based on Rodgers diffusion factor equation [33].

$$b_2 = \frac{10(D_2 - D_1)}{1 + (w_2/w_1)} \left[ \frac{D_f - 1 + \frac{w_2}{w_1}}{\frac{\pi D_2 u_2 \psi_w}{2 Z_b L_0 w_1}} \right] - \frac{(D_{s1} - D_{h1})}{2} \quad (3)$$

The diffusion factor ( $D_f$ ) is estimated using Jansen model [34] which determines the diffusion as a function of flow deceleration and turning.

$$D_f = 1 - \frac{W_2}{W_{1s}} + \frac{0.75 \Delta h_{Euler} / u_2^2}{\left( \frac{W_{1s}}{W_2} \right) \left[ \left( \frac{Z_b}{\pi} \right) \left( 1 - \frac{D_{1s}}{D_2} \right) + 2 \frac{D_{1s}}{D_2} \right]} \quad (4)$$

The first term of equation (4) is related to the flow diffusion due to the reduction in average velocity while the second section is related to the loading distribution on the blade [35].

Based on the diffusion factor; Rodgers [33] derived a formula to correlate the initiation of stall with the limitation in the impeller diffusion capability.

$$\frac{\varphi_{ch}}{\varphi_{stall}} \approx \frac{1}{\left( 1.05 - D_f \right) \left[ 1 + \psi_w M u^2 \left( \frac{k-1}{2} \right) \right]^{1/(k-1)}} \quad (5)$$

Kim et al. [21] introduced design procedures of the conventional vane and low solidity vane diffusers system aiming to achieve a wider flow range for centrifugal compressor stage. Another design method was developed for channel diffusers by Kalinkevych and Skoryk [26] according to the given velocity distribution and based on the solving of the gas dynamic inverse problem.

According to Kalinkevych and Skoryk model [26], the flow rate in vane diffuser is calculated based on the fundamental continuity equation:

$$\dot{m} = \eta \cdot \varepsilon(\eta) \cdot a_{cr} \cdot \rho^* \cdot 2\pi \cdot r \cdot b \cdot \left[ 1 - \frac{(\delta_v + \sum \delta^*) Z_v}{2\pi r \sin \alpha} \right] \cdot \sin \alpha \quad (6)$$

Where:

$\eta$ : Velocity coefficient (vm/acr)

$\varepsilon(\eta)$ : Gas dynamic function of density

$a_{cr}$ : Critical sonic speed

$\rho^*$ : Stagnation density

The gas dynamic functions of density ( $\varepsilon(\eta)$ ) and pressure ( $\pi(\eta)$ ) can be defined in terms of gas properties as following:

$$\varepsilon(\eta) = \frac{\rho}{\rho^*} = \left(1 - \frac{k-1}{k+1} \eta^2\right)^{1/(k-1)} \quad (7)$$

$$\pi(\eta) = \frac{p}{p^*} = \left(1 - \frac{k-1}{k+1} \eta^2\right)^{k/(k-1)} \quad (8)$$

The vaned diffuser throat blockage factor ( $\tau$ ) measures the ratio between ineffective flow area  $\left(1 - \frac{A_E}{A}\right)$  to the total area ( $A$ ). This is determined by formula (8) as a function of vane thickness ( $\delta_v$ ) and number of vanes ( $Z_v$ ) based on Kalinkevych et al. model [25].

$$\tau = 1 - \left[ \frac{2\pi r_3 \sin(\alpha_3) - \left(\delta_v + \sum \delta^*\right) Z_v}{2\pi r_3 \sin(\alpha_3)} \right] \quad (9)$$

Where:

$\sum \delta^*$ : Total displacement thickness of boundary layers

Therefore, by substituting equation (7), the equation (6) can be written in a new form:

$$\dot{m} = 2v_m \rho \pi r b \cdot \left[ 1 - \frac{\left(\delta_v + \sum \delta^*\right) Z_v}{2\pi r \sin \alpha} \right] \sin \alpha. \quad (10)$$

For purpose of simplicity, the effect of boundary layer will be ignored in this study. For linear pressure distribution along the vane pitch, the average flow velocity ( $\eta$ ) can be calculated in terms of velocities on the vane suction ( $\eta_{ss}$ ) and pressure surfaces ( $\eta_{ps}$ ).

$$2\pi(\eta) = 2\pi(\eta_{ss}) + \pi(\eta_{ps}) \quad (11)$$

The presence of the flow separation zone at the pressure side of vaned diffuser vane causes the effective area of the flow channel to decrease leading to higher flow velocity and friction losses. Therefore, the prediction of pre-separation condition of the boundary layer and using flow separation control will help to improve the stage characteristics.

The velocity distribution at pressure surface can be predicted using the below equation.

$$\eta_{ps} = \eta_1 \left[ 1 + \frac{(\bar{l} - \bar{l}_1) \cdot (2 + H_s) \cdot (-f_s)}{\bar{\delta}_1^{**}} \right]^{-1(2+H_s)} \quad (12)$$

Where:

$\bar{\delta}^{**}$ : Relative momentum thickness  $= \frac{\delta_1^{**}}{L_v}$

$L_v$ : Vane centerline length.

$l$ : Vane centerline length coordinate.

$H_s, f_s$ : Boundary layer shape parameters.

The recommended value of boundary layer shape parameter ( $f_s$ ) is -0.02 while the value of coefficient ( $H_s$ ) varies between 2.4 and 3.0.

The impeller exit blockage factor ( $\tau_{IEB}$ ) is calculated using the derived equation by Okhuaesogie et al. [36].

$$\tau_{IEB} = 1 - \left[ \frac{2\pi r_2 \sin(\alpha_2) h_{b2} - 0.5(\delta_{h2} + \delta_{s2}) h_{b2} Z_v}{2\pi r_2 \sin(\alpha_2)} \right] \quad (13)$$

Where:

$\delta_{h2}$ : Blade thickness at impeller exit hub.

$\delta_{s2}$ : Blade thickness at impeller exit shroud.

$h_{b2}$ : Blade height at impeller exit.

Since the vaneless space is designed to reduce the high velocity of the discharge flow from the impeller, the leading edge radius of the diffuser ( $r_3$ ) can be estimated using equation (14) based on the flow Mach number ( $M_2$ ) and exit flow angle ( $\alpha_3$ ) [21].

$$\frac{r_3}{r_2} = \frac{1 + \alpha_3}{360} + \frac{Mu_2^2}{15}. \quad (14)$$

The vane passage length ( $L_v$ ) is determined according to the divergence angle ( $\theta_d$ ), number of vanes ( $Z_v$ ), inlet and exit radius and vane angle. The equivalent divergent angle is used to account the flow diffusion losses and it is modelled using the two-dimensional diffuser analogy.

$$L_v = \pi \frac{r_4 \sin \beta_4 - r_3 \sin \beta_3}{Z_v \tan \theta_d}. \quad (15)$$

For low solidity vane diffusers with straight vanes, the vane length ( $L_v$ ) is calculated by equation (16). This model has been proposed by Kim et al. [21].

$$L_v = 2r_3 \sin\left(\frac{180}{Z_v}\right) \cos\left(\beta_3 + \left(90 - \cos^{-1}\left[\sin\left(\frac{180}{Z_v}\right)\right]\right)\right). \quad (16)$$

The exit blade angle ( $\beta_4$ ) is specified to satisfy the maximum allowed solidity without forming a throat using equation (17). This value is then substituted in equation (18) to define the optimum exit diffuser radius.

$$\beta_4 = \tan^{-1} \left[ \tan \beta_3 + \frac{2 \sin(180/Z_v)}{\cos \beta_3} - \frac{\delta_3}{2r_3 \sin \beta_3} \right]. \quad (17)$$

$$r_4 = r_3 \frac{\cos \beta_3}{\cos \beta_4}. \quad (18)$$

The maximum allowed solidity at no throat conditions is determined using equation (19).

$$\sigma_{\max} = \frac{\left(l + \frac{\delta_3}{2 \tan \beta_3}\right)}{2r_3 \sin\left(\frac{180}{Z_v}\right)}. \quad (19)$$

There are two basic parameters are used to measure the diffuser performance: blade loading parameter (BL) and static pressure recovery coefficient (PRC).

$$BL = \frac{2\pi(r_3 v_{\theta 3} - r_4 v_{\theta 4})}{Z_v L_v (v_{m3} - v_{m4})}. \quad (20)$$

$$PRC = \frac{p_4 - p_3}{p_{03} - p_3}. \quad (21)$$

The limits of divergent angle ( $\theta_d$ ) and blade loading parameter (BL) were specified by Aungier [37] to avoid the diffuser stall and to achieve the maximum static pressure recovery.

$$2\theta_d \leq 11^\circ. \quad (22)$$

$$BL \leq \frac{1}{3}. \quad (23)$$

The pressure loss across the diffuser passage is derived using Stanitz[38] model assuming a compressible flow with friction and heat transfer but without considering of the mixing losses.

$$\Delta h = C_p T_{03} \left[ \left( \frac{P_4}{P_{04}} \right)^{(\gamma-1)/\gamma} - \left( \frac{P_4}{P_{03}} \right)^{(\gamma-1)/\gamma} \right]. \quad (24)$$

However, the main cause of this loss is the fluid friction with the diffuser surface so that the higher flow velocity or the longer flow surface leads to greater loss. Although that the increase in the exit diffuser radius reduces the flow velocity, it also yields to a higher flow length which is one of the contributed factors to the diffuser loss.

### 3. Developed Approach Description

There are several available models in the open literature which define the design procedures for vaneless and vaned diffusers, but generally they are depending on the detailed geometrical features of the diffuser system and require a calibration with experimental data. The established model aims to derive the characteristics and energy coefficients of the diffuser system assuming different configurations as demonstrated in Figure 1. This can be used then to evaluate the appropriate diffuser type for such duty by analysing its impact on stage efficiency and flow range. The fundamental principle of the developed method is based on the determination of potential effect of diffuser geometrical features and inlet conditions on diffuser system characteristics. This defined by five key parameters which are: diffuser inlet Mach number ( $Mu_3$ ), inlet vane ( $\beta_3$ ) and flow angles ( $\alpha_3$ ), number of vanes ( $Z_v$ ) and dimeter ratio ( $r_4/r_3$ ).

The inlet width of vaneless diffuser ( $b_3$ ) is estimated according to the specified inlet configuration and based on the calculated exit impeller width ( $b_2$ ) from equation (25). The diffusion factor of the impeller is obtained by Jansen model [34].

$$b_3 = PP\% \times \left[ \frac{10(D_2 - D_1)}{1 + (w_2/w_1)} \right] \left\{ \left[ 1 - \frac{W_2}{W_{1s}} + \frac{0.75 \Delta h_{Euler} / u_2^2}{\left( \frac{W_{1s}}{W_2} \right) \left[ \left( \frac{Z_b}{\pi} \right) \left( 1 - \frac{D_{1s}}{D_2} \right) + 2 \frac{D_{1s}}{D_2} \right]} \right] \right. \quad (25)$$

$$\left. - 1 + \frac{w_2}{w_1} - \frac{\pi D_2 u_2 \psi_w}{2 Z_b L_\theta w_1} - \frac{(D_{s1} - D_{h1})}{2} \right\}$$

Where:

PP%: Pinched percentage

The diffuser diameter ratio ( $D_4/D_3$ ) is set at the beginning based on the recommended range (1.25-1.6). This value is iterated later to satisfy the demanded stage pressure ratio at the design point. The exit flow velocity is determined as a function of the diameter ratio and it is then used to obtain the exit absolute Mach number and flow coefficient. The gas properties are assumed to be constant at the beginning as the inlet values. This allows

to derive the first iteration pressure ratio and accordingly the stage discharge parameters. In the second iteration, the obtained discharge pressure is compared with the required at design conditions and the diameter ratio is reviewed accordingly.

Moreover, the physical gas properties are recalculated using the new discharge pressure and temperature values. In the case of conventional vaned diffuser, the blockage factor at inlet throat is obtained by equation (9). Furthermore, the velocity distribution is determined according to Kalinkevych and Skoryk model [26].

The number of vanes is set based on the standard values. The selection of the optimum diffuser vanes number is complicated due its aerodynamic interaction with the impeller and volute. However, it is necessary to check that the diffuser vanes number is less than the number of impeller blades in order to avoid the early stalling. This is caused by the diffuser passage blockage by the initiated wakes at the impeller exit blades. Furthermore, the surge flow tends to increase as the number of vanes increases due to unsteady distribution of the flow near vanes which creates a kind of obstruction for the incoming flow to the diffuser.

For low solidity vane diffuser, the exit vane angle is determined assuming straight vanes with the maximum allowed solidity at no throat conditions. This is then substituted in equation (18) to obtain the exit diffuser diameter ( $D_4$ ). The same procedures are then applied to derive the performance parameters of the centrifugal compressor stage. Therefore, the obtained performance curves of each diffuser configuration at various flow coefficients are optimized to select the optimum design based on stage efficiency and operating range.

### 4. Results and Discussion

The vaneless region in this study is referred to the space between the impeller exit and the diffuser throat which is critical to guide the impeller flow to the diffuser and to ensure an effective diffusion process. This gap serves to reduce the diffuser inlet Mach number and to settle the flow before reaching the leading edge of diffuser vane. However, this space is not a basic part since there are some compressors are designed without this gap. For better performance, it is important to consider the right size since the large space leads to increase overall radial size and the boundary layer growth which in turn yields to a flow blockage in the diffuser while the excessive short space causes a high level of noise, vibration and stresses.

**Table 1. Characteristics of the Investigated Stage Diffuser**

Design Parameter	Value
Inlet Diffuser Pressure (kpa)	886
Inlet Diffuser Temperature (°k)	331
Mass Flow Rate (kg/s)	55.9
Number of Diffuser Vanes	16
Inlet Diffuser Radius (mm)	327.5
Outlet Diffuser Radius (mm)	527.0
Width of Diffuser (mm)	53.2

The geometrical features of the investigated centrifugal compressor stage are shown in Table 1. Figure 2 illustrates the variation of the overall stage pressure ratio and efficiency at different diameter ratios. The larger diameter

size of the vaneless space enhances the static pressure recovery of the discharge gas from the impeller leading to greater pressure ratio. This is owing to the higher diffusion factor which increases proportionally with the diameter ratio. However, the normalized efficiency trend demonstrates a reduction in the overall efficiency value at large diameter size despite the continuous rise in the stage pressure ratio. This sort of behaviour can be elucidated by

looking to the pressure loss coefficient curve in Figure 2 which clearly shows that the pressure losses are increasing proportionally with the diameter ratio. Furthermore, the pressure loss trend is taking a greater slope as the diameter ratio increases. This in fact yields to a higher pressure loss coefficient rise comparing with the static pressure recovery increase leading in turn to lower overall stage efficiency.

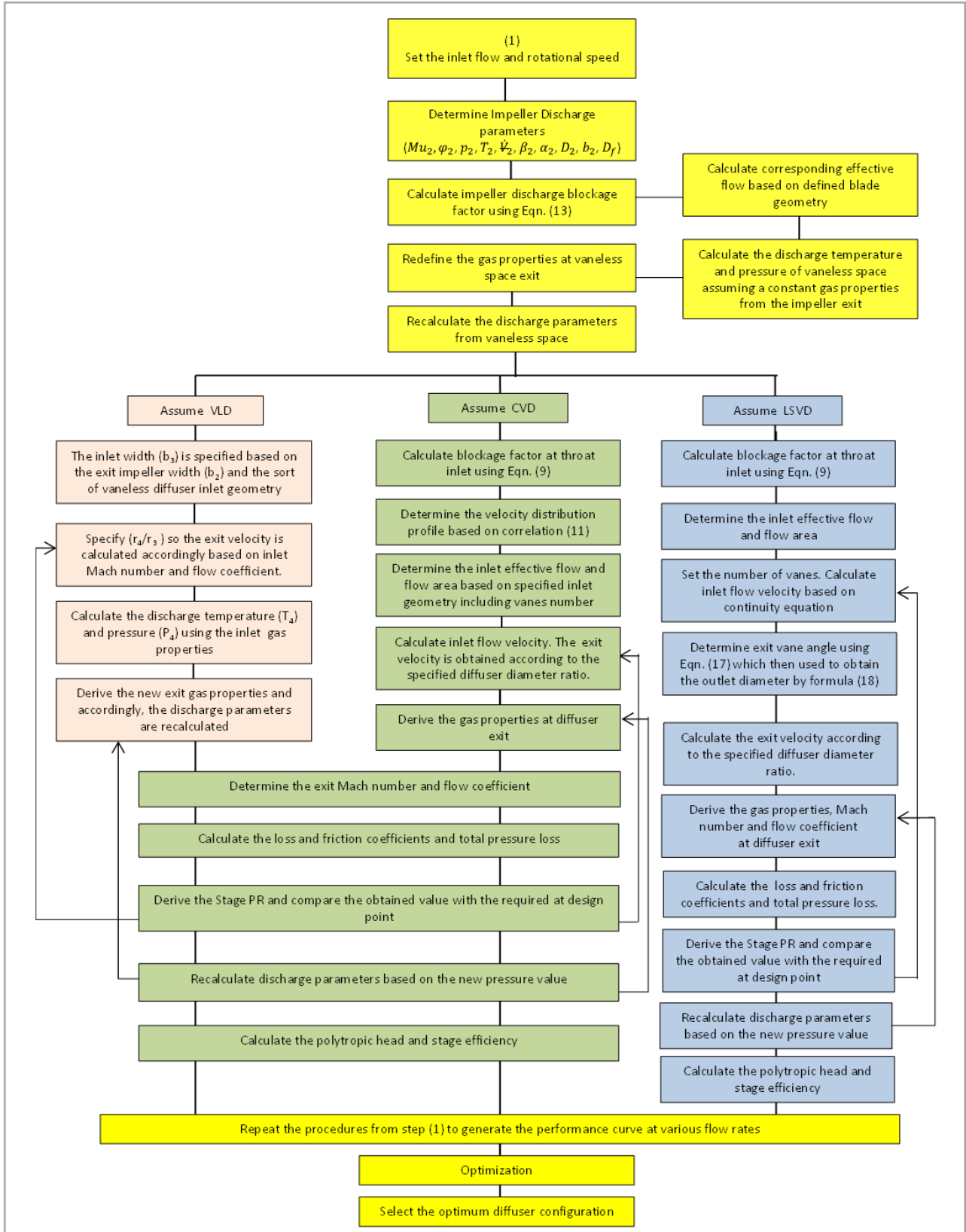


Figure 1. Developed Method to Evaluate the Diffusion System Performance

Two of the main parameters which have influence on the diffuser pressure losses are the friction factor ( $\lambda_{fr}$ ) and exit blade angle ( $\beta_2$ ). Figure 3 shows the effect of friction factor on the pressure loss coefficient at various diameter ratio and fixed blade exit angle.

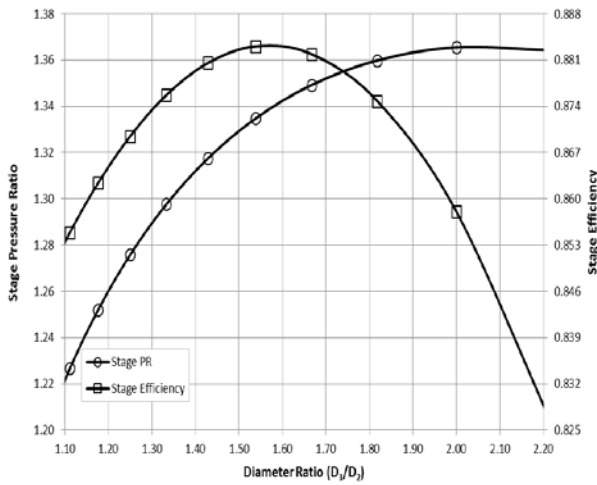


Figure 2. Effect of Vaneless Space Diameter on Stage Efficiency and Pressure Ratio

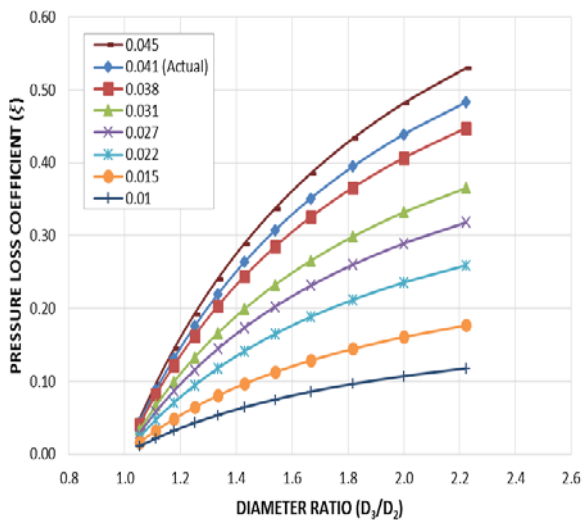


Figure 3. Determination of Vaneless Space Loss at Various Diameter Ratio and Friction Factors

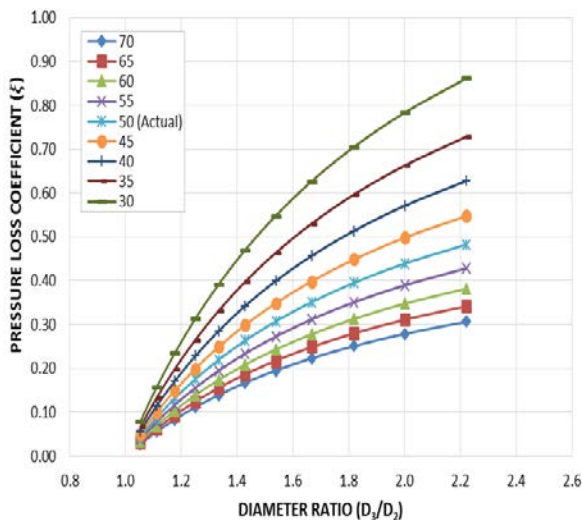


Figure 4. Determination of Vaneless Space Loss at Various Diameter Ratio and Blade Exit Angles

When there is a need for large gap size, the high associated pressure losses can be reduced by decreasing the friction factor which can be controlled by considering the surface roughness of the vaneless space. Moreover, Figure 4 demonstrates that the exit blade angle has more significant effect on the pressure loss coefficient due to its influences on the flow unsteadiness at impeller discharge. At high exit blade angle, the flow enters the vaneless diffuser at larger flow angle ( $\alpha_2$ ) so that the associated pressure losses in the downstream vaneless space are reduced substantially especially at large diameter ratios. Therefore, the optimum blade angle has to be selected to consider the best fit with the diffuser size.

For further investigation on the effect of diffuser configuration on stage efficiency and operating range, six different diffuser schemes have been studied as shown in Figure 5. The first four diffusers are having conventional vaned diffuser configuration and with different number of vanes.

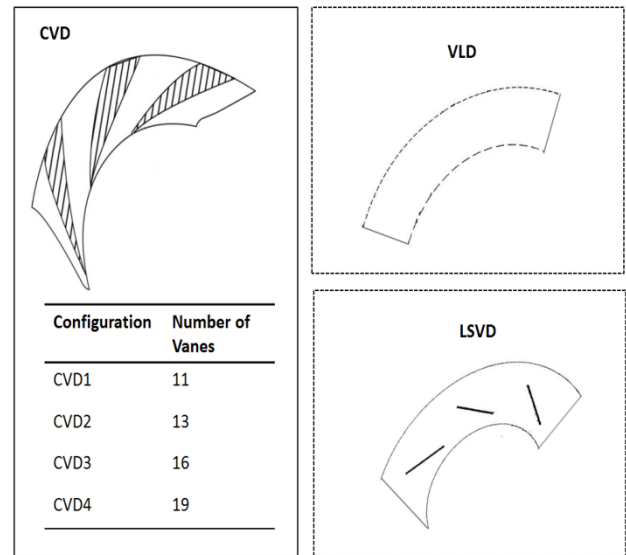


Figure 5. The Configurations of the Studied Diffusers

In order to determine the velocity at the inlet and exit of each diffuser, the velocity distribution at suction and pressure sides of each diffuser vanes surfaces along the flow channel is predicted using Kalinkevych and Skoryk model [26]. These will be then used to calculate the average velocity at each diffuser inlet and exit. To determine the boundary layer shape factors ( $f_s, H_s$ ), an iteration process is first of all performed to match the predicted velocity profile of the studied diffuser configuration (Table 2) with the estimated values. After several trials, Figure 6 illustrates the closest predicted velocity distribution to the actual profile at  $f_s$  and  $H_s$  of -0.02 and 2.8 respectively which will be used for the rest of diffusers.

Figure 7 shows the estimated velocity distribution along the channel vaned diffuser for four various configurations. It is clear that the velocity at suction and velocity sides of the diffuser vane surface is decreasing as the vanes number increases. However, it is interesting to observe that the difference between the velocities profiles becomes more significant at suction surface of the diffuser vane. This in fact indicates the impact of diffuser geometry on the aerodynamic interaction with the impeller discharge.

**Table 2. Characteristics of the Studied Diffuser by Kalinkevych et al. [26]**

Design Parameter	Value
Inlet Diffuser Pressure (kpa)	118
Inlet Diffuser Temperature (°k)	319
Mass Flow Rate (kg/s)	1.775
Number of Vanes	17
Inlet Diffuser Radius (mm)	262
Outlet Diffuser Radius (mm)	309
Width of Diffuser (mm)	15.5

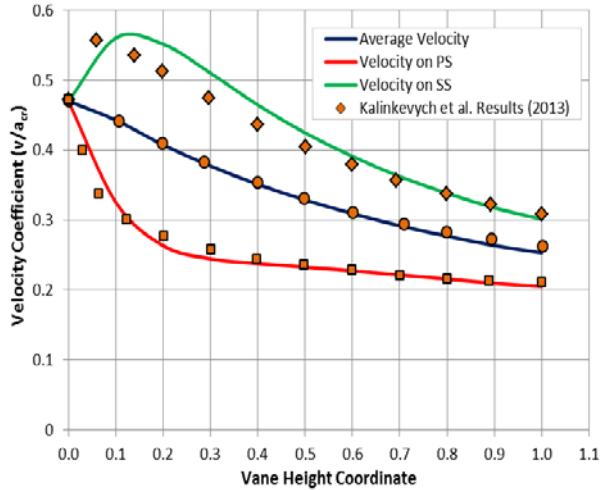


**Figure 6. Prediction of Boundary Layer Shape Factors of Kalinkevych-Skoryk Model [26]**

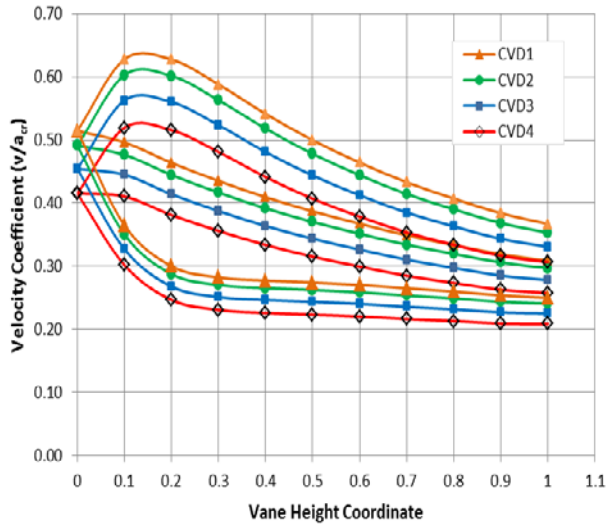


**Figure 7. Predicted Velocity Distribution at Suction and Pressure Diffuser A Long the Flow Path of Studied Conventional Diffusers Configurations**

The smaller available flow area of CVD4 reduces the gas velocity at vanes suction. Moreover, the low velocity at vanes pressure side demonstrates a greater static pressure recovery as the vanes number increases. The highest average velocity was obtained from CVD1 while the minimum was found at CVD4. This can be also confirmed by the Mach number trend in Figure 8. The diffuser CVD1 has the highest absolute Mach number at the diffuser exit comparing with the rest of diffusers. As aforementioned, this indicates a lower diffusion factor and less static pressure recovery. Besides, the Mach number tends to increase further at high flow rates.

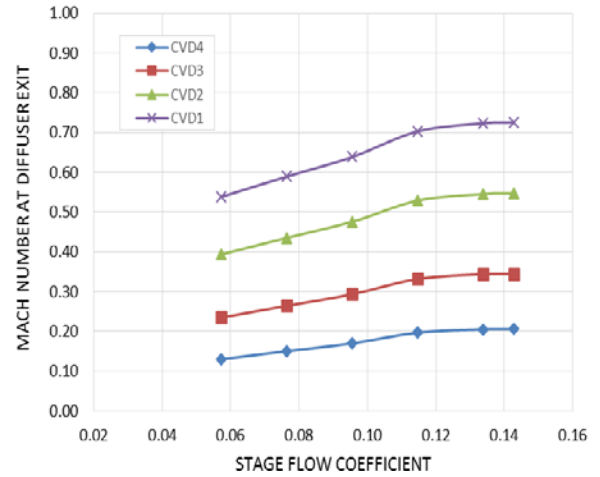


**Figure 8. Obtained Absolute Mach Number at Vaned Diffuser Exit**

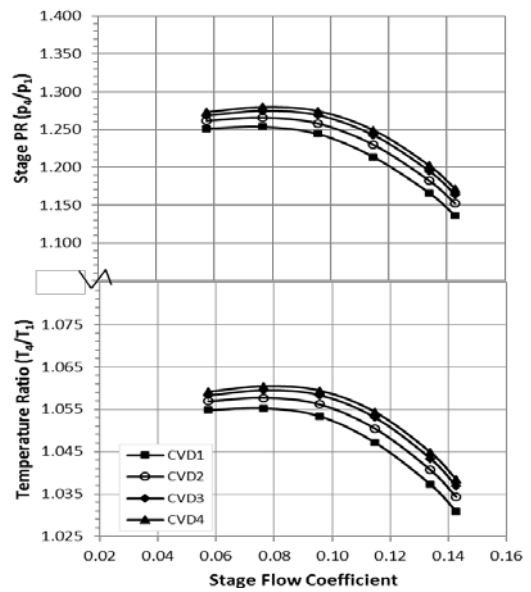


**Figure 9. Predicted Normalized Stage Pressure and Temperature Ratios at Various Vaned Diffuser Configurations**

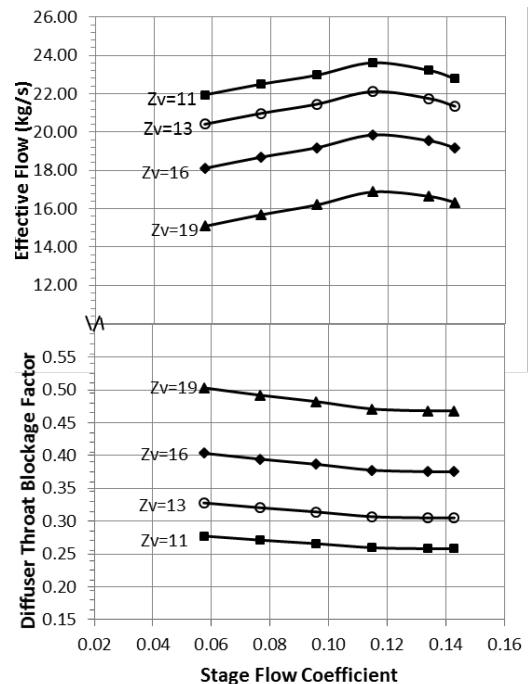


**Figure 10. Predicted Blockage Factor and Effective Flow at Various Vaned Diffuser Configurations**

In terms of stage pressure ratio, the predicted overall pressure ratio at various vaned diffuser configurations are plotted in Figure 9 at various flow coefficients. The vanes are designed to increase and control the diffusion rate and then reduce the losses. The high number of vanes in CVD4 allows for greater static pressure recovery throughout the diffuser channel which leads to greater overall pressure ratio. However, the effect of vanes number on pressure ratio becomes less substantial as the number of vanes increases. This is due to the fact that the number of diffuser vanes started to exceed the impeller blades number leading to greater flow distortion and throat diffuser blockage as shown in Figure 10.

The diffuser blockage factor is increasing proportionally with the vanes number and it reached the highest value at CVD4. This blockage effect is created due to the local boundary layer and the formation of throat area. The blockage factor was also found greater at low flow coefficients due to the higher flow distortion at diffuser inlet. For a given inlet temperature and pressure to the leading edge of diffuser vanes, the effective mass flow is specified based on the throat area of the diffuser passage. Therefore, the high blockage factor at high vanes number limits the available effective flow area. This obviously leads to reduce the effective flow through the diffuser channel gradually as shown in Figure 10.

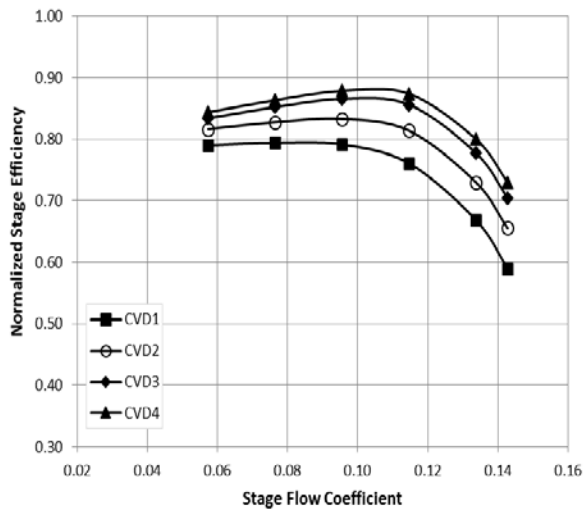


Figure 11. Predicted Stage Efficiency with Various Vaned Diffuser Configurations

The impact of diffuser vanes number is also illustrated in Figure 11 and Figure 12 in terms of stage efficiency and operating range. The high static pressure recovery at larger vanes number leads to raise the stage efficiency due to lower frictional losses as shown in Figure 11. However, this impact on stage efficiency becomes less significant at high vanes number due to substantial increase in the pressure losses. At surge condition and as the number of diffuser vanes increases, the pressure recovery coefficient of the vaneless space is reduced with more distorted velocity distribution. Figure 12 compares the obtained surge margin and overload percentage at various diffuser configurations. It is clear that there is a slight increase in the choke flow as the vanes number increases. On the other hand, the effect on surge flow was found more significant leading to reduce the flow range dramatically at high vanes number. A reduction by about 3.41% was

recorded in the surge margin when the diffuser configuration is changed from CVD1 to CVD4 by an average drop of approximately 0.43% for every diffuser vane.

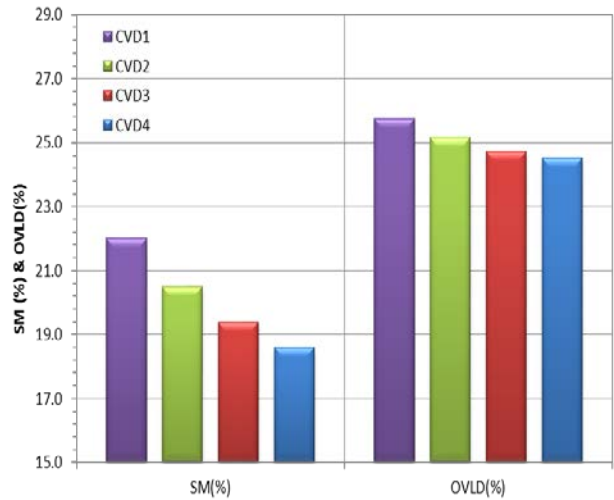


Figure 12. Predicted Operating Range at Various Vaned Diffuser Configurations at Design Flow

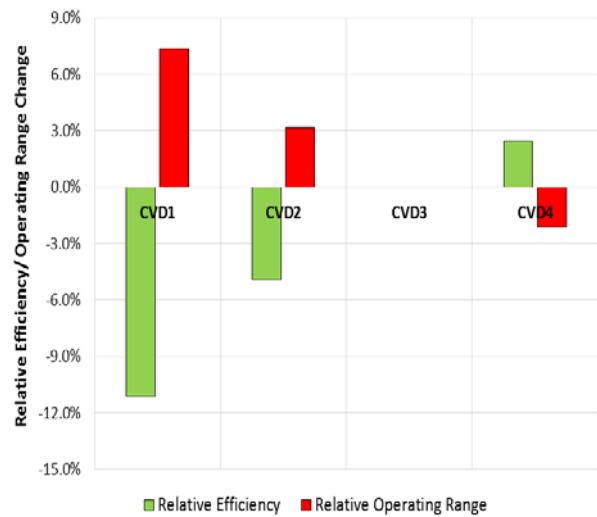


Figure 13. Comparison Between Predicted Change in Efficiency and Stability

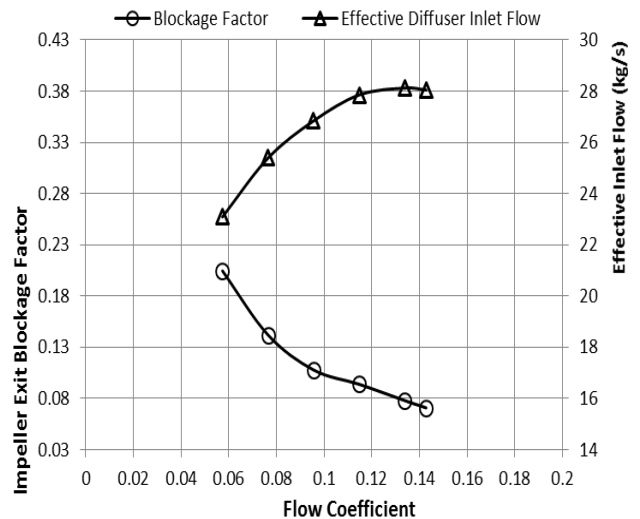


Figure 14. Predicted Impeller Exit Blockage Factor and Inlet Effective Flow of Vaneless Diffuser (VLD)

The surge generally occurs when the incoming flow gets obstructed by the friction near vanes. As the number of vanes increases, it becomes difficult to divide the working gas equally between the diffuser passages. So, when the inlet flow drops at constant speed, the amount of flowing gas through each passage decreases. Consequently, the inlet relative velocity and flow angle are reduced causing an excessive positive incidence at the leading edge of the diffuser vane. This in turn leads to increase the length of the flow path spiral thus, the flow momentum at the diffuser walls is dissipated by friction and stall. Figure 13 shows the relative change in the efficiency and operating range with respect to the reference design (CVD3). More pronounced effect was observed in the determined polytropic efficiency based on overall stage total-to-total conditions. By upgrading the diffuser design to CVD4, the stage efficiency was improved by roughly 2.4% over the initial design. However, this was achieved in expenses of about 2.1% reduction in the stable flow range. More significant rise in the operating range can be achieved by reducing the diffuser vanes number to 13 by around 3.1% against 4.9% drop in stage efficiency.

The proposed approach was also used to evaluate the stage characteristics with different diffuser types including: vaneless diffuser (VLD), vaned diffuser (CVD3) and low solidity vaned diffuser (LSVD). Figure 14 demonstrates the obtained blockage factor of vaneless diffuser (VLD) at impeller discharge which indicates the distortion rate of impeller exit flow profile. The high incidence angle at low flow coefficients causes the blockage factor to increase due to the growth of boundary layer separation. This agrees with the obtained trend in Figure 10 for the diffuser throat blockage factor in vaned diffuser. However, the determined inlet effective flow is higher in this type of diffuser due to reduction in the created blocked area by boundary layer growth and throat area formation. The blockage factor is approximately 9% at design flow. This in fact can be used as an indication of late stall comparing with the vaned diffuser.

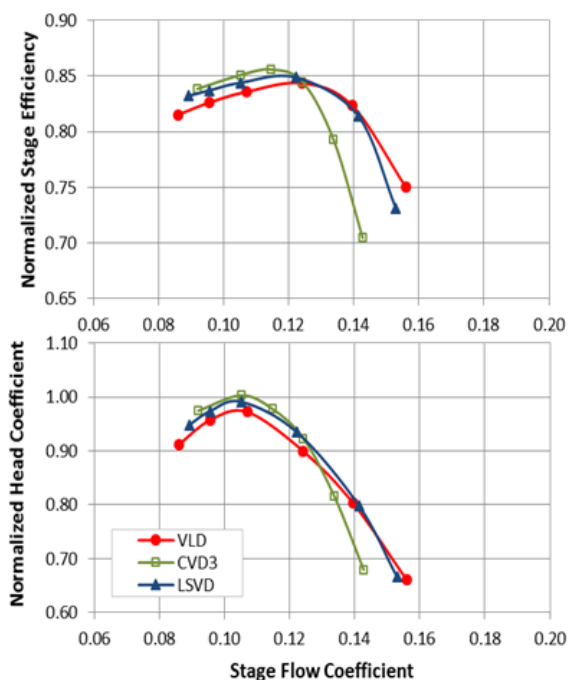


Figure 15. Comparison Between Normalized Stage Efficiency and Head Coefficient of Various Diffuser Types At Design Speed

Figure 15 compares the determined normalized head coefficient and stage efficiency of various diffuser configurations at design rotational speed. The head coefficient of the LSVD stage is very close to the CVD stage and both are higher than the determined head by VLD stage. The peak efficiency of the CVD3 is the greatest among the studied configurations. The absence of vanes in the vaneless diffuser leads to increase the moved particle distance through a vaneless diffuser yielding to a higher wall friction and greater kinetic energy loss. However, the minimum mass flow of the CVD3 stage is approximately 6.9 % greater than the VLD. Moreover, the LSVD has quite well efficiency over a wide flow range comparing with the VLD but slightly lower than the CVD3. Besides, the behaviour of LSVD performance curve at overload flow range is similar to the VLD and it was not affected substantially by the higher negative incidence angles as the conventional vaned diffuser. The peak efficiency of LSVD was attained at higher flow rate than with the CVD3.

Furthermore, it was observed that the vaneless diffuser stage has relatively a flatter speed line near the peak efficiency point and the peak efficiency occurred at higher flow coefficient than CVD3 and LSVD. From head coefficient curve in Figure 15, the CVD3 has the highest head coefficient comparing with LSVD and VLD but with earlier stall. One noticeable aspect of the LSVD performance is its reduced head coefficient rise to the surge. At low flow rates, the efficiency of VLD decreases dramatically because of flow separation and rotating stall inception. Figure 16 illustrates the predicted surge margin and overload range for the three different diffuser configurations. This has been predicted using correction factor method based on the measured performance characteristics by Hohlweg et al. [39]. The vaned diffuser tends to stall at higher flow coefficient and with limited overload flow range. Thus, it has the shortest flow range comparing with the other configurations. The high positive incidence at the leading edge of the CVD3 vane at low flow rates brings the stage to stall condition. The recorded relative drop in the surge margin of CVD3 was about 5.63% with relative to VLD. This difference is reduced in the case of LSVD to approximately 2.83%.

One of the basic parameters which influence the LSVD performance is the inlet vane angles as shown in Figure 17 and Figure 18.

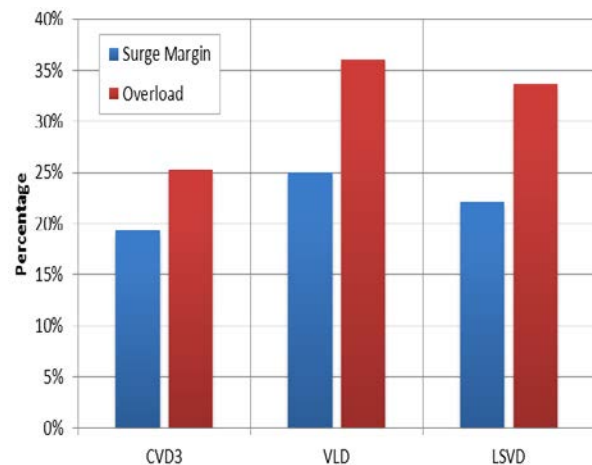


Figure 16: Comparison Between Operating Range of Various Diffuser Types At Design Speed

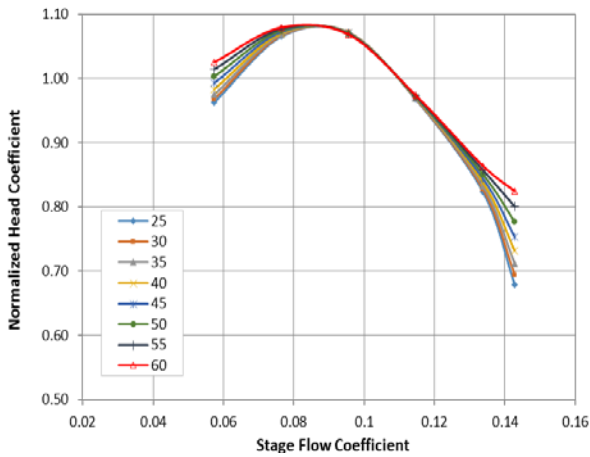


Figure 17. Effect of Inlet Vane Angle on the Normalized Head Coefficient of LSVD Stage

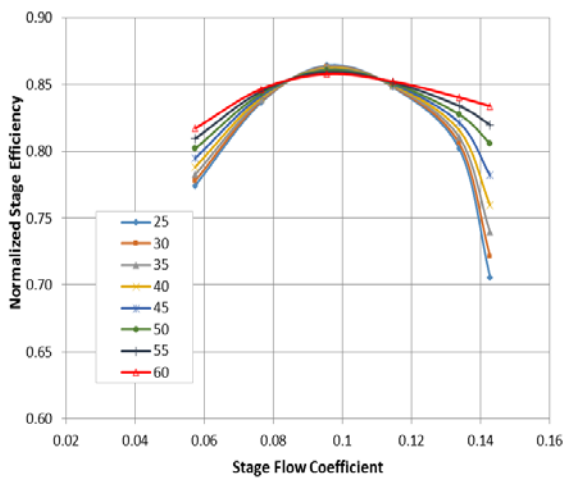


Figure 18. Effect of Inlet Vane Angle on the Normalized Polytropic Efficiency of LSVD Stage

Table 3. Effect of Inlet Vane Angle on Operating Range of LSVD Stage

$\beta_3(^{\circ})$	SM (%)	OVL D (%)
25.0	19.516	24.750
30.0	19.990	25.028
35.0	20.551	25.269
40.0	21.196	25.477
45.0	21.912	25.654
50.0	22.685	25.805
55.0	23.490	25.932
60.0	24.300	26.037

It was observed that there is no significant impact of the vane leading edge angle on the head coefficient and polytropic efficiency at normal stable operating range. However, the impact of changing the inlet vane angle becomes more substantial near the surge and choke limits. The inlet vane angle affects the flow distortion at the diffuser inlet especially at very high and low flow rates. The high inlet angle causes the change in the speed line to be flatter as the operating point approaches the stable flow range ends leading to less reduction in the stage efficiency and head coefficient. However, the speed lines of high inlet vane angle have relatively lower peak efficiency and this drop in the peak efficiency increase as the inlet angle goes up. On the other hand, these is a positive effect of high inlet vane angle on the stage operating range as shown in Table 3. It is clear that the surge margin and

overload range are increasing proportionally with the vane angle rise. This basically explains the advantage of using adjustable LSVD in order to compromise between the effect of inlet vane angle on peak efficiency and stable flow range.

Economically, the performance of the diffuser can be plotted in terms of cumulative power loss as shown in Figure 19. Despite the fact that the manufacturing cost of the vaneless diffuser is the lowest, the cumulative cost of power loss is the highest among the other configuration. This is influenced by the project lifetime. Therefore, the total power loss cost has to be optimized and balanced with the total manufacturing cost.

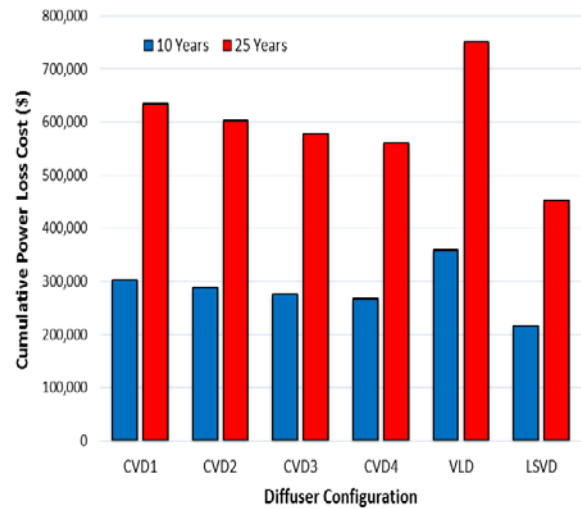


Figure 19: Cost Estimation of Diffuser Power Loss for Different Configuration at Power Cost of \$0.06/kWh

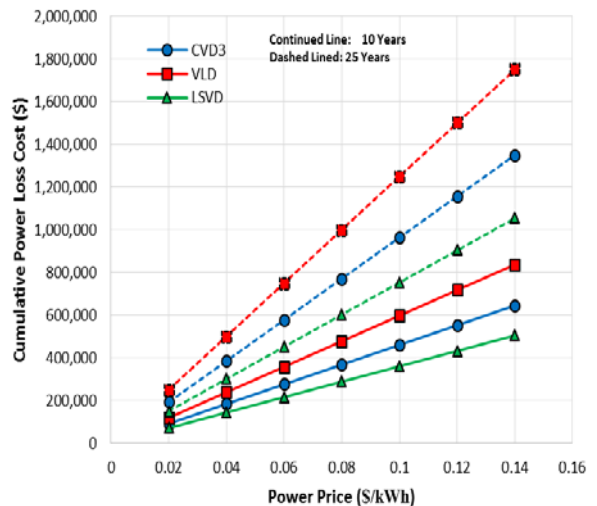


Figure 20. Cost Estimation of Diffuser Power Loss for Different Configuration at Various Power Price Rate

However, the derived figure is for one mechanical stage, so this power loss cost will be obviously much greater while dealing with multi-stages compressor. Moreover, the lowest power loss cost was observed with low solidity vaned diffuser as a result of high overall operating efficiency. An interesting point is that the difference between the power loss cost of the tested conventional diffusers (CVD1, CVD2, CVD3, CVD4) are close to each other due to the negative effect of flow blockage at high vanes number. The power rate cost is another factor which has a direct impact on the economic value of the studied

diffuser configurations. Figure 20 illustrates the predicted cost of diffuser loss at various power prices. More substantial effect can be observed at high power price. Therefore, this graph can be used as general guideline to select the optimum diffuser configuration according to the existing power cost rate and based on the specified project lifetime. For multi-stages compressors, the determined value can be roughly multiplied by the number of stages to estimate the overall value.

## 5. Conclusion

This paper introduced an empirical approach to evaluate the diffuser characteristics of centrifugal compressor stage based on multi-decision optimization process. The technical evaluation has been conducted to analyze the impact of diffuser features on operating efficiency and stable flow range. On the other hand, the economic analysis has been performed to investigate the influences of the selected geometrical features of the diffuser on the economic viability of the compression system in terms of power loss cost.

It was found that the high associated pressure losses with the large vaneless space size can be reduced by decreasing the friction factor which can be controlled by considering the surface roughness of the vaneless space. However, more significant effect on the diffuser pressure loss coefficient was recorded by controlling the impeller exit blade angle due to its influences on the flow unsteadiness at impeller discharge. Moreover, the performed comparison revealed that low solidity vaned diffuser has quite well efficiency over a wide flow range comparing with the vaneless diffuser but slightly lower than the conventional vaned diffuser. Besides, the vaned diffuser tends to stall at higher flow coefficient and with limited overload flow range. Thus, it has the shortest flow range comparing with the other configurations. The high positive incidence at the leading edge of the conventional vaned diffuser vane at low flow rates brings the stage to stall condition. The recorded relative drop in the surge margin of conventional vaned diffuser was about 5.63% and 2.83% with relative to vaneless diffuser and low solidity vaned diffusers, respectively.

From economic perspective, the cumulative cost of power loss of vaneless diffuser is the highest among the other configuration. However, this has to be balanced with the total capital cost and the project lifetime in order to make the optimum decision. However, the difference between the power loss cost of the tested conventional diffusers are close to each other despite the variety in the manufacturing cost due to the negative effect of flow blockage at high vanes number. Thus, for higher long-term economic performance, it is not sufficient to select the characteristics of diffuser geometry based on the low manufacturing cost or efficiency improvement criterion only.

## Acknowledgements

Special thanks to Petroleum Development Oman Company and Cranfield University for supporting this study.

## Nomenclature

A Area

$\beta$	Blade/Vane Angle
$V$	Absolute Velocity
$\eta$	Efficiency
$b_2$	Impeller Exit Blade Width
$\rho$	Density
$r$	Radius
$D$	Diffuser Diameter
$D_f$	Diffusion Factor
$w$	Relative Velocity
$Z_v$	Number of Vanes
$k$	Specific Heats Ratio
$u_2$	Impeller Exit Tip Velocity
$\psi_w$	Work Coefficient
$\delta$	Blade/Vane Thickness
$\sum \delta^*$	Total Displacement Thickness of Boundary Layers
$P_0$	Total Pressure
$T_0$	Total Temperature
$\Delta h$	Enthalpy Drop
$C_p$	Specific Heat Capacity
$L_\theta$	Blade Meridional Length
$2\theta_d$	Divergent Angle
$L_v$	Vane Length
$Mu$	Mach Number
$\alpha$	Flow Angle
$a_{cr}$	Critical Velocity
$\xi$	Loss Coefficient
$\lambda_{fr}$	Friction Coefficient
$h_b$	Blade Height
$\varphi$	Flow Factor
$Re$	Reynolds Number
$H_s, f_s$	Boundary Layer Shape Parameters
$\varepsilon(\eta)$	Gas Dynamic Functions of Density
$\pi(\eta)$	Gas Dynamic Functions of Pressure
$\sigma_{max}$	Maximum Solidity
$\tau$	Vaned Diffuser Throat Blockage Factor
$\tau_{IEB}$	Impeller Exit Blockage Factor

## Subscripts

0	Total
1	Impeller Inlet
2	Impeller Outlet
3	Vaneless Space Exit
4	Diffuser Exit
d	Design Conditions
h	Hub
$ps$	Pressure Side
$s$	Shroud
$ss$	Suction Side
$t$	Tip
$v$	Vaness
$m$	Radial Component
$\theta$	Tangential Component

## Abbreviations

LSVD	Low Solidity Vaned Diffusers
PP	Pinched Percentage
PR	Pressure Ratio
VD	Vaned Diffuser

VLD	Vaneless Diffuser
SM	Surge Margin $\left( SM = \frac{\varphi_d - \varphi_{surge}}{\varphi_d} \right)$
OVL	Overload Margin $\left( OVL = \frac{\varphi_{choke} - \varphi_d}{\varphi_d} \right)$
OR	Operating Range
BL	Blade Loading Coefficient
ch	Choke

## References

- [1] L. F. Schumann, (1985), A Three-Dimensional Axisymmetric Calculation Procedure for Turbulent Flows in a Radial Vaneless Diffuser, Paper No. 85-GT-133, ASME, New York.
- [2] Yingkang, Z. and Sjolander, S. (1987), Effects of Geometry on the Performance of Radial Vaneless Diffuser, Journal of Turbomachinery, 109:550-556.
- [3] Aungier, R. H. (1988), A Performance Analysis For The Vaneless Components Of Centrifugal Compressors, Flows In Non-Rotating Turbomachinery Components, ASME FED-Vol 69, 1988, pp. 35-43.
- [4] Y. Tsujimoto, Y. Yoshida, and Y. Mori (1996), Study of Vaneless Diffuser Rotating Stall Based on Two-Dimensional Inviscid Flow Analysis, Journal of Fluids Engineering, vol. 118, no. 1, pp. 123-127, 1996.
- [5] H. S. Dou and S. Mizuki (1996), Analysis of the Flow in Vaneless Diffusers with Large Width-to-Radius Ratios. In ASME 1996 International Gas Turbine and Aeroengine Congress and Exhibition (pp. V001T01A098-V001T01A098). American Society of Mechanical Engineers.
- [6] Yu-Tai Lee, Lin Luo and Thomas W. Bein (2001), Direct method for optimization of a centrifugal compressor vaneless diffuser, New York, ASME/2000-GT-453.
- [7] S. Ljevar, H. C. de Lange and A. A. Van Steenhoven (2006), Vaneless diffuser core flow instability and rotating stall characteristics. In Institution of Mechanical Engineers, Fluid Machinery Group-Ninth European Fluid Machinery Congress. UK: Institution of Mechanical Engineers (pp. 379-389).
- [8] C. Gao, C. Gu, T. Wang, and Z. Dai (2008), Numerical analysis of rotating stall characteristics in vaneless diffuser with large width-radius ratio, Frontiers of Energy and Power Engineering in China, vol. 2, no. 4, pp. 457-460.
- [9] H. Tamaki (2013), Study on flow fields in high specific speed centrifugal compressor with unpinched vaneless diffuser, Journal of Mechanical Science and Technology, vol. 27, no. 6, pp. 1627-1633.
- [10] M. Kalinkevych and O. Shcherbakov (2013), Numerical Modeling of the Flow in a Vaneless Diffuser of Centrifugal Compressor Stage, ISRN Mechanical Engineering, 2013.
- [11] A. N. Abdelhamid (1983), Effects of Vaneless Diffuser Geometry on Flow Instability in Centrifugal Compression Systems, Canadian Aeronautics and Space Journal, vol. 29, no. 2, pp. 259-266.
- [12] Y. Kinoshita and Y. Senoo (1985), Rotating Stall Induced in Vaneless Diffusers of Very Low Specific Speed Centrifugal Blowers, Journal of Engineering for Gas Turbines and Power, vol. 107, no. 2, pp. 514-521, 1985.
- [13] A. Jaatinen-Varri, P. Roytta, T. Turunen-Saaresti, and A. Gronman (2013), Experimental Study of Centrifugal Compressor Vaneless Diffuser Width, Journal of Mechanical Science and Technology, vol. 27, no. 4, pp. 1011-1020.
- [14] R. Aungier (1988), A Systematic Procedure for the Aerodynamic Design of Vaned Diffusers. ASME FED, 69, 27-34.
- [15] Y. Yoshinaga, I. Gyobu, H. Mishina, F. Koseki and H. Nishida (1980), Aerodynamic Performance of a Centrifugal Compressor With Vaned Diffusers, Transaction of ASME, vol. 102, 486-493.
- [16] C. Rodgers (1982), The performance of centrifugal compressor channel diffusers, New York, ASME-82-GT-10.
- [17] U. Haupt, U. Seidel, A. N. Abdul-Hamid and M. Rautenberg (1988), Unsteady Flow in a Centrifugal Compressor with Different Types of Vaned Diffusers, New York: American Society of Mechanical Engineers, ASME/88-GT-22.
- [18] Kim, W. and Engeda, A. (1997), Comparison of Pressure Recovery and Overall Performance of Different Diffusers for Centrifugal Compressor, In FEDSM97-3029 Fluids Engineering Division Summer Meeting, ASME.
- [19] F. Justen, K. U. Ziegler and H. E. Gallus (1999), Experimental investigation of unsteady flow phenomena in a centrifugal compressor vaned diffuser of variable geometry, New York, ASME, ASME/98-GT-368.
- [20] N. He and A. Tourlidakis, (2001), Analysis of Diffusers with Different Number of Vanes in a Centrifugal Compressor Stage, In 2001-GT-0321, ASME TURBO EXPO.
- [21] Kim, Y., Engeda, A., Aungier, R., & Amineni, N. (2002), A centrifugal compressor stage with wide flow range vaned diffusers and different inlet configurations, Proceedings of the Institution of Mechanical Engineers, Part A: Journal of Power and Energy, 216(4), 307-320.
- [22] A. Engeda (2003), Experimental and Numerical Investigation of the Performance of a 240 kW Centrifugal Compressor with Different Diffusers, Experimental Thermal and Fluid Science, 28(1), 55-72.
- [23] T. Turunen-Saaresti (2004), Computational and Experimental Analysis of Flow Field in the Diffusers of Centrifugal Compressors, PhD thesis, Lappeenranta University of Technology.
- [24] J. Issac, N. Sitaram, and M. Govardhan (2004), Effect of Diffuser Vane Height and Position on the Performance of a Centrifugal Compressor, Proceedings of the Institution of Mechanical Engineers, Part A: Journal of Power and Energy, 218(8):647-654.
- [25] M. Kalinkevych, O. Obukhov, A. Smirnov, and A. Skoryk (2011), The design of vaned diffusers of centrifugal compressors based on the given velocity distribution, in Proceedings of the 7th International Journal of Rotating Machinery 7 International Conference on Compressors and their Systems, pp. 61-69, Woodhead Publishing, 2011.
- [26] M. Kalinkevych and A. Skoryk (2013), Design Method for Channel Diffusers of Centrifugal Compressors, International Journal of Rotating Machinery.
- [27] T. C. S. Reddy, G. R. Murty and MVSSM. Prasad (2014), Effect of diffuser vane shape on the performance of a centrifugal compressor stage, Journal of Thermal Science, 23(2), 127-132.
- [28] C. Osborne, and J. Sorokes (1988), The Application of Low Solidity Diffusers in Centrifugal Compressors, Flows in Non-Rotating Turbomachinery Components, ASME FED-Vol 69, pp. 89-101.
- [29] J. M. Sorokes and J. P. Welch (1991), Centrifugal Compressor Performance Enhancement Through the Use of Single-Stage Development Rig, In Proceedings of the 20th Turbomachinery Symposium, Texas A&M (pp. 101-112).
- [30] .M. Sorokes, and J.P. Welch (1992), Experimental Results on a Rotatable Low Solidity Vaned Diffuser, ASME Preprint 92-GT-19.
- [31] Y. Galerkin, K. Soldatova and O. Solovieva, (2015), Numerical Study of Centrifugal Compressor Stage Vaneless Diffusers, In IOP Conference Series: Materials Science and Engineering (Vol. 90, No. 1, p. 012048), IOP Publishing.
- [32] Cheng Xu and Ryoichi. S. Amano (2012), Empirical design considerations for industrial centrifugal compressors, International Journal of Rotating Machinery, vol. 2012 (2012), Article ID: 18406.
- [33] C. Rodgers (1978), A Diffusion Factor Correlation for Centrifugal Impeller Stalling, 78-GT-61.
- [34] W. Jansen (1967), A method for Calculating the Flow in a Centrifugal Impeller When Entropy Gradients are Present, Institution of Mechanical Engineers, Royal Society Conference on Internal Aerodynamics (Turbomachinery ), pages: 133-146.
- [35] Barend W. Botha and Adriaan Moolman (2005), Determining the Impact of the Different Losses on Centrifugal Compressor Design, R & D Journal, 2005, 21 (3) incorporated into The SA Mechanical Engineer.
- [36] O.F. Okhuahesogie, J. Stewart, F.J.G. Heyes and P.E. Roach (2012), Design Optimization of Two-Stage Turbocharger Compressor Impeller, KTP Associates Conference, University of Brighton, UK, 14 June 2012.
- [37] R. Aungier (1997), Design of Centrifugal Compressor Stage for Enhanced Operating Range and Head Rise, Internal Report (Cited in Kim et al., 2002).
- [38] Stanitz JD (1952), Some Theoretical Aerodynamic Investigations of Impellers in Radial and Mixed-Flow Centrifugal Compressors, Cleveland, Ohio, Transactions of the ASME, Vol. 74, 473-476.
- [39] Hohlweg, W. C., Drenzi, G. L., & Aungier, R. H. (1993, May), Comparison of Conventional and Low Solidity Vaned Diffusers, In ASME 1993 International Gas Turbine and Aeroengine Congress and Exposition (pp. V001T03A039-V001T03A039). American Society of Mechanical Engineers.